Zinc Binding Properties of the DNA Binding Domain of the 1,25-Dihydroxyvitamin D_3 Receptor†

Theodore A. Craig,‡ Timothy D. Veenstra,‡ Stephen Naylor,§,||,⊥,# Andy J. Tomlinson,||,⊥ Kenneth L. Johnson,||,⊥ Slobodan Macura,|| Nenad Juranić,|| and Rajiv Kumar*,‡,§,||

Nephrology Research Unit, Departments of Medicine, Biochemistry and Molecular Biology, Biomedical Mass Spectrometry Facility, Department of Pharmacology and Clinical Pharmacology Unit, Mayo Clinic and Foundation, Rochester, Minnesota 55905

Received March 12, 1997; Revised Manuscript Received June 25, 1997⊗

ABSTRACT: To assess the zinc binding stoichiometry and the structural changes induced upon the binding of zinc to the human vitamin D receptor (VDR), we expressed the DNA binding domain (DBD) of the human VDR in bacteria as a soluble glutathione-S-transferase fusion protein at 20 °C, and examined the apo-protein and metal-liganded protein by mass spectrometry, and circular dichroism and nuclear magnetic resonance spectroscopy. Following final preparation with a zinc-free buffer, the VDR DBD bound 2 mol of zinc/mol of protein as measured by inductively coupled plasma-mass spectrometry and electrospray ionization-mass spectrometry. When protein preparation was carried out in a zinc containing buffer and zinc content of the protein was assesed by the same methods, VDR DBD bound 4 mol of zinc/mol of protein. Analysis of the protein using circular dichroism spectroscopy demonstrated that the EDTA-treated protein increased in α-helical content from 16 to 27% on the addition of zinc. Equilibrium ultracentrifugal analyses of the VDR DBD indicated that the protein was present in solution as a monomer. Gel mobility shift analyses of the VDR DBD with several vitamin D response elements (VDREs) in the absence of accessory proteins such as retinoic acid receptor, showed that VDR DBD was able to form a protein/VDRE DNA structural complex. In the presence of zinc, proton NMR NOESY spectra showed that the protein possessed elements of secondary structure. The addition of VDRE DNA, but not random DNA, caused changes in the proton NMR spectra of VDRE DNA indicating specific interaction between protein and DNA groups. We conclude that the DBD of the VDR binds zinc and DNA and undergoes conformational changes on binding to the metal and DNA.

Vitamin D_3, via its active metabolite 1,25-dihydroxyvitamin D_3, plays a vital role in mineral homeostasis, cellular growth, and development (Darwish & DeLuca, 1993; Holick, 1995; Kumar, 1990, 1991; Lowe et al., 1992). Many of the effects of 1,25-dihydroxyvitamin D_3 are mediated by an intracellular receptor, the 1,25-dihydroxyvitamin D_3 receptor (frequently abbreviated as the vitamin D receptor or VDR)[1] (Darwish & DeLuca, 1993; Pike, 1991; Schwabe & Rhodes, 1991; Carlberg, 1996). The human VDR (hVDR) is an ∼48 kDa ligand-dependent transcription factor which is structurally related to other members of the steroid/thyroid superfamily of nuclear receptors. It is comprised of discrete DNA and ligand binding domains. The DNA binding domain of the VDR has putative "zinc finger" regions which are believed to bind to unique DNA sequences in the promoter regions of vitamin D-responsive genes. In many cases, the VDR binds to DNA response elements of vitamin D-responsive genes as a heterodimer with other nuclear DNA binding proteins such as the retinoic acid X-receptor, thereby positively or negatively exerting control of gene transcription (Darwish & DeLuca, 1993). In other instances, the VDR binds to DNA sequences as a homodimer (Freedman & Towers, 1991; Carlberg et al., 1993; Mangelsdorf et al., 1995; Darwish & DeLuca, 1993).

Studies on the chemical and structural properties of the VDR have been hampered by the lack of large amounts of the biologically active protein. In particular, there is no information on the zinc binding properties of the DNA binding domain of the VDR. It is not known whether the addition of zinc causes the protein to undergo a change in conformation as might be expected if the protein bound zinc in a specific manner. There is no direct information about the secondary structure of the DNA binding domain of the VDR. Furthermore, it is not known whether the protein undergoes structural changes upon binding to DNA response elements in vitamin D-responsive genes. Such changes would be expected to occur if the protein were to bind specifically to DNA.

To clarify many of the issues noted above, we expressed the DNA binding domain of the vitamin D receptor in soluble

† Supported by National Institutes of Health Grant DK25409.

* Address correspondence to Mayo Clinic, 200 First St., SW, 911A Guggenheim Bldg., Rochester, MN 55905. Phone: 507-284-0020. Fax: 507-266-4710. E-mail: rkumar@mayo.edu.

‡ Nephrology Research Unit.

§ Department of Medicine.

|| Department of Biochemistry and Molecular Biology.

⊥ Biomedical Mass Spectrometry Facility.

Department of Pharmacology and Clinical Pharmacology Unit.

⊗ Abstract published in *Advance ACS Abstracts,* August 15, 1997.

[1] Abbreviations: VDR, 1,25-dihydroxyvitamin D_3 receptor; DBD, DNA binding domain; VDRE, vitamin D response element; GST, glutathione-S-transferase; ESI-MS, electrospray ionization-mass spectrometry; MALDI-MS, matrix-assisted laser desorption/ionization-mass spectrometry; MRE, mean residue ellipticity; ICP-MS, inductively coupled plasma-mass spectrometry; OP, osteopontin; OC, osteocalcin; DR3, direct repeat 3 VDRE; DR3′, direct repeat 3′ VDRE; CD, circular dichroism; NMR, nuclear magnetic resonance; NOESY, nuclear Overhauser enhancement spectroscopy.

S0006-2960(97)00561-8 CCC: $14.00

form in a bacterial expression system. We examined the zinc binding properties of the VDR DBD by mass spectrometry and the structural properties of the protein by analytical ultracentrifugation, circular dichroism, and nuclear magnetic resonance spectroscopy.

MATERIALS AND METHODS

General. Ultraviolet spectroscopy was carried out using a Beckman DU-70 spectrophotometer (Beckman Instruments, Inc., Fullerton, CA). Sodium dodecyl sulfate−polyacrylamide gel electrophoresis (SDS−PAGE) was carried out as described (Laemmli, 1970) using a PhastSystem (Pharmacia Biotech, Inc., Piscataway, NJ). Low-temperature protein expression in *Escherichia coli* was accomplished using a temperature-controlled New Brunswick shaking incubator (Edison, NJ). The original human vitamin D receptor clone was obtained from Dr. J. W. Pike (Ligand Pharmaceuticals, San Diego, CA). 1,25-dihydroxyvitamin D_3 was a gift of Dr. Milan Uskokovic (Hoffman LaRoche, Nutley, NJ). Western blots were carried out after electrophoretic transfer to nitrocellulose (Schleicher & Schuell, Keene, NH) (Towbin et al., 1979) using rabbit polyclonal antibody made against bacterially expressed full-length hVDR (Kumar et al., 1992). Protein purification was carried out with a Mono S HR 5/5 or 10/10 column (Pharmacia) and a Waters 650E Advanced Protein Purification System (Waters division of Millipore, Milford, MA).

Polymerase Chain Reaction (PCR) Amplification and Cloning of the DNA Binding Domain of hVDR. An ca. 350 base pair PCR product encompassing the coding region for amino acids 1−110 of hVDR was prepared using the cDNA for full-length hVDR. Two PCR primers were synthesized to obtain an hVDR PCR product incorporating *Bam*HI and *Sal*I restriction sites (Innis et al., 1990). The 5′ primer included a *Bam*HI restriction site (underlined) and the 3′ primer included a *Sal*I restriction site (underlined):

5′ primer:
5′ AGGGATCCATGGAGGCAATGGCGGCCAGCACTT
3′ [33 mer]

3′primer:
5′ ATTGTCGACTCACCGCTTCAGGATCATCTC
3′ [33 mer]

The ∼350 bp PCR product was purified by agarose electrophoresis and was cloned into pCRII (Invitrogen, Carlsbad, CA). The 1−110 hVDR/pCRII construct was cleaved with *Bam*HI and *Sal*I and the insert DNA was ligated into *Bam*HI/*Sal*I cleaved pGEX-4T-2, the *Schistosoma japonicum* glutathione-S-transferase fusion protein expression vector (Pharmacia, Piscataway, NJ). The ligated construct was used to transform *E. coli* DH5α cells. Plasmids prepared from this host were subsequently used to transform *E. coli* BL21 cells for protein expression.

Large-Scale Expression and Purification of VDR DBD. Large-scale expression and batch purification of the VDR DBD was carried out essentially as described for the ligand binding domain of hVDR except as noted (Craig & Kumar, 1996). Briefly, a single colony was inoculated into 2× YTA (with ampicillin 100 μg/mL) and grown overnight. Starter cultures (5 mL) were inoculated into 500 mL 2× YTA/2 L flask and grown at 37 °C with shaking at 360 rpm, until OD_{600nm} was ∼1. Isopropyl thio-β-D-galactoside (IPTG) was added to 0.1 mM in order to induce protein expression. The incubator temperature was immediately changed to 20 °C, and the cells were grown for another 12 h. Cells were harvested by centrifugation and cell pellets were frozen or used immediately for protein preparations.

Cell pellets were resuspended in PBS-DTT-Zn buffer (140 mM NaCl, 2.7 mM KCl, 10 mM Na_2HPO4, 10 mM DTT, 40 μM $ZnCl_2$, pH to 7.3 with NaOH) containing 5 mM EDTA (approximately 50 g fresh weight cells/40 mL final volume). A 30 min egg lysozyme treatment (1 mg/ml) was used for some preparations prior to sonication. Phenylmethanesulfonyl fluoride was added to 4 mM, and cells were sonicated on ice for 12 min. Homogenates were clarified by centrifuging them twice at 30000*g* at 4 °C for 20 min. The supernatant was combined with 17 mL of bed volume Glutathione Sepharose-4B (Pharmacia) in 50 mL tubes and mixed on a rotating wheel for 1.5 h at 4 °C. The tube was centrifuged at 1000*g* at 4 °C for 5 min, and the supernatant was discarded. The resin was washed sequentially eight times by resuspension and centrifugation with 50 mL PBS-DTT (no $ZnCl_2$)/6 mL resin and then eight times with TD-Zn buffer (50 mM Tris, 10 mM DTT, 40 μM $ZnCl_2$, pH 8.0). The resin was transferred to a column and washed again with PBS-DTT-Zn and then with TD-Zn buffer. The 1−110 hVDR/GST fusion protein was eluted from the resin at 4 °C by serial additions of glutathione elution buffer (50 mM Tris, 10 mM DTT, 10−25 mM glutathione, 120 mM NaCl, pH 8.0). Bovine thrombin (500 units) (Sigma T-7513, St. Louis, MO) was added and allowed to cleave the 1−110 VDR from the GST for several days at 4 °C or until SDS−PAGE analysis indicated that thrombin cleavage was complete.

The partially purified 1−110 VDR thrombin digest was further purified by Mono S chromatography. A Mono S HR 10/10 (Pharmacia) column was used with a programmed gradient of 0 to 1 M NaCl in TD buffer (50 mM Tris, 10 mM DTT, pH 8.0, at 20 °C) at a flow rate of 4 mL/min. The gradient was developed as follows: hold buffer without NaCl for 5 min following loading of the sample; gradient 0 to 0.1 M NaCl over 5 min; gradient 0.1 to 0.15 M NaCl over 15 min; hold 0.15 M NaCl 10 min; gradient 0.15 to 0.2 M NaCl over 10 min; hold 0.2 M NaCl 15 min; gradient 0.2 to 1.0 M NaCl over 25 min; hold 1.0 M NaCl 15 min before reequilibrating column to 0 M NaCl. VDR DBD eluted at ∼0.4 M NaCl following the programmed wash steps. Column fractions with pure protein as judged by SDS−PAGE were combined and extensively dialyzed against TD-Zn (100 μM $ZnCl_2$) and stored at 4 °C or frozen.

Measurement of Zinc Stoichiometry by Inductively Coupled Plasma-Mass Spectrometry. Aliquots of VDR DBD in TD-Zn (100 μM $ZnCl_2$) were dialyzed against TD alone (sample volume to buffer volume was 1:2000) for 4 days at 4 °C using a 1000 MW cut off Spectra/Por dialysis membrane (Spectrum Medical Industries, Houston, TX). After the first day, the protein sample was dialyzed for another 3 days using new dialysis membrane and fresh buffer. Gel filtration analyses were done by passing VDR DBD samples in TD-Zn (100 μM $ZnCl_2$) serially over two NAP25 columns (Pharmacia). Buffer without protein was processed similarly. Zinc concentrations and amino acid composition were determined in pooled fractions of pure protein following dialysis or chromatography. For controls, the same fractions

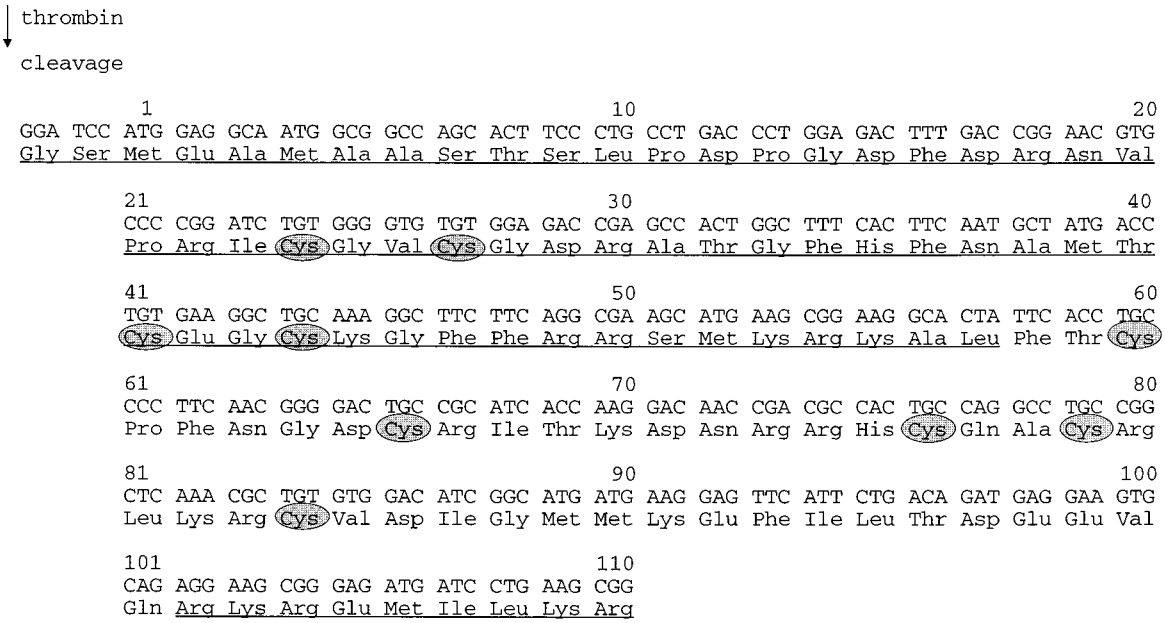

FIGURE 1: DNA and amino acid sequence of the DNA binding domain of the human vitamin D receptor. The DNA sequence of the coding region of VDR DBD and of the amino acid sequence of the purified construct following thrombin cleavage of the GST fusion protein are shown. Numbers refer to VDR amino acids. Underlined amino acids indicate regions of the protein verified by amino acid sequencing starting from either the amino-terminal or carboxyl-terminal end of the protein. The nine Cys in VDR DBD are shown (shaded). The first eight Cys make up the putative "zinc finger" regions in structures of related proteins.

were pooled from a blank Mono S chromatographic separation performed without protein. Dialysis or blank buffers were also taken for zinc determination. Zinc determinations were carried out using a Perkin-Elmer SCIEX inductively coupled plasma-mass spectrometer model 5000A (Foster City, CA).

Electrospray Ionization-Mass Spectrometry of Apo- and Metal-Bound VDR DBD. Electrospray ionization-mass spectrometry (ESI-MS) measurements were performed on a Finnigan MAT 900 spectrometer (Bremen, Germany), a double focusing instrument of EB geometry. ESI measurements were done in the positive ion mode using a Finnigan MAT electrospray interface. Protein solutions were introduced into the ESI source via 50 μm i.d. fused silica line, using a 50 μL syringe and a Harvard Apparatus model 22 syringe pump (South Natick, MA). The flow rate of sample introduction was 0.2 μL/min. An instrument resolution of approximately 1000 was used for the analyses. The instrument was scanned from mass to charge (m/z) 600−3000 at a rate of 10 s/mass decade. Calibrations of the m/z axis were done in the positive ion mode with liquid secondary ion mass spectrometry using clusters of cesium iodide as the reference. The position and time-resolved ion counter array detector was used for ion detection. Multiple scans were recorded and summed by the instrument data system (Finnigan MAT ICIS software, version 8.01HB). Multiply charged spectra were deconvoluted to afford a molecular weight (M_r) using algorithms supplied with the instrument data system. Samples for ESI-MS were prepared as follows: Samples of zinc-free VDR DBD (Figure 3A) were prepared from VDR DBD in TD-Zn (100 μM $ZnCl_2$) by adsorbing the protein on a small reversed phase protein precolumn (Michrom BioResources Inc., Auburn, CA). The adsorbed protein was rinsed with 50 μL of water/acetonitrile/glacial acetic acid (90/10/2, v/v/v), then with 50 μL of water before eluting with 10 μL of acetonitrile/n-propanol/water/glacial acetic acid (55/10/35/0.6, v/v/v/v). The 10 μL of eluant containing VDR DBD

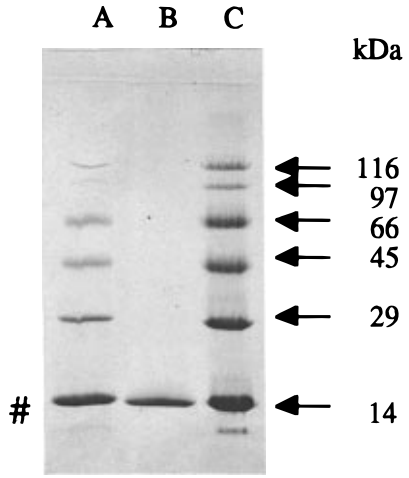

FIGURE 2: SDS−polyacrylamide gel electrophoresis of VDR DBD. SDS−PAGE gel of VDR DBD (#) following Mono S purification (lane B). MW standards (lanes A and C).

was then diluted with 90 μL of 4 mM NH_4HCO_3, pH 8.0, containing 15% methanol, and the sample was introduced into the ESI source. Samples of VDR DBD in buffer without zinc (Figure 3, panels B and C) were prepared by extensively dialyzing VDR DBD in TD-Zn (100 μM $ZnCl_2$) against 4 mM NH_4HCO_3, 1 mM DTT, pH 8.3, before introducing the protein into the ESI source in the same buffer. A zinc acetate solution was added for zinc loaded samples. Sample concentration varied from 8 to 36 μM protein.

Matrix-Assisted Laser Desorption/Ionization-Mass Spectrometry (MALDI-MS). MALDI-MS was carried out on VDR DBD exchanged into 50 mM NH_4HCO_3, pH 7.5. A Bruker Biflex mass spectrometer (Billerica, MA) was used for the analyses with either α-cyano-4-hydroxycinnamic acid or 3,5-dimethoxy-4-hydroxycinnamic acid as matrix. A nitrogen laser at 337 nm was used throughout. Lys-C protease digests of VDR DBD were prepared as follows: VDR DBD in 50 mM Tris, 10 mM DTT, 100 μM $ZnCl_2$,

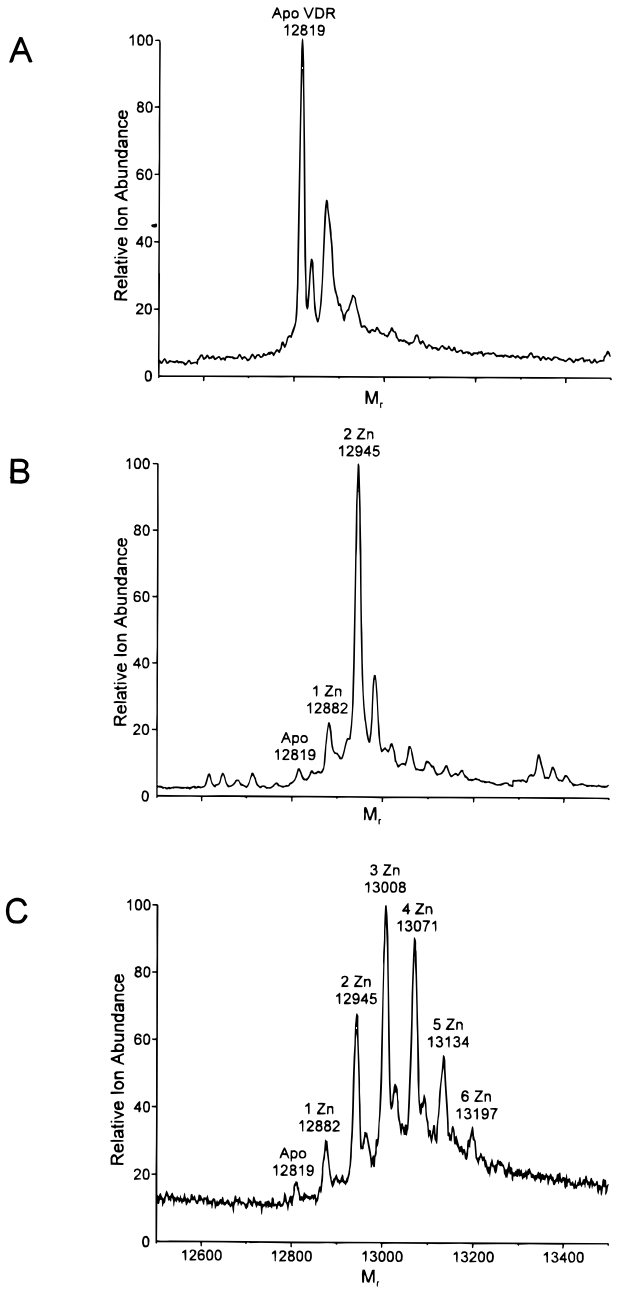

FIGURE 3: Zinc binding to VDR DBD by electrospray ionization-mass spectrometry (ESI-MS). (Panel A) Deconvoluted ESI-MS spectrum of apo-VDR DBD. 0 Zn^{2+}, M_r = 12 819 Da. Panel B: Deconvoluted ESI-MS spectrum of VDR DBD prepared in the presence of Zn^{2+} and exchanged into 4 mM NH_4HCO_3, 1 mM DTT, pH 8.3 (see Materials and Methods). 2 Zn^{2+}, M_r = 12 945; 1 Zn^{2+}, M_r = 12 882; 0 Zn^{2+}, M_r = 12 819. (Panel C) Deconvoluted ESI-MS spectrum of VDR DBD after addition of 50-fold excess of zinc. M_r for the following peaks: 0 Zn^{2+}, 12 819 Da; 1 Zn^{2+}, 12 882 Da; 2 Zn^{2+}, 12 945 Da; 3 Zn^{2+}, 13 008 Da; 4 Zn^{2+}, 13 071 Da; 5 Zn^{2+}, 13 134 Da; 6 Zn^{2+}, 13 197 Da.

pH 8.0, was reduced with DTT (10-fold molar excess) for 20 min at at room temperature. The protein was alkylated by addition of iodoacetamide (10-fold molar excess) for 20 min at room temperature. Reduction and alkylation steps were repeated followed by further addition of DTT before the sample was reduced to dryness under vacuum. The sample was reconstituted in 100 mM Tris-HCl, pH 8.25. A 3 h digestion at 37 °C with Lys-C protease (2% w/w; enzyme/protein) was carried out. Time-of-flight measurements were used to determine the sizes of proteolytic products for comparison to sizes from expected proteolytic cuts.

DNA Sequencing and Protein Characterization. The DNA sequence of the entire coding sequence of VDR was verified by dideoxy DNA sequencing of both strands of plasmid minipreps (Sanger et al., 1977). Amino acid compositions on the VDR DBD protein were carried out using the method of Bidlingmeyer et al. (1984). Amino-terminal protein sequencing was carried out on a Perkin-Elmer/Applied Biosystems 492 Procise protein sequencer while carboxyl-terminal sequencing was done on a Perkin Elmer/Applied Biosystems 492C Procise protein sequencer (Foster City, CA).

Circular Dichroism Studies. Circular dichroic measurements of the VDR DBD were recorded on a JASCO J-710 spectropolarimeter equipped with a data processor. The VDR DBD was zinc depleted by treatment with 50 mM EDTA at pH 5.5 in 25 mM sodium acetate, 1 mM DTT overnight. The sample was then exhaustively dialyzed against pH 5.5 buffer with 10 μM EDTA and concentrated with a Centricon-3 microconcentrator (Amicon, Beverly, MA). The protein was zinc depleted to ~0.5 mol of zinc/mol of the VDR DBD. Measurements were made at 22 °C in 25 mM sodium acetate, 10 μM EDTA, 1 mM DTT (pH 5.5), using a quartz cell with a path length of 0.49 mm. A total of 10 scans were recorded and averaged for each sample. All resultant spectra were baseline subtracted. To monitor the effect of Zn^{2+} on the conformation of the VDR DBD, protein samples were recorded in the presence of 0, 10, 20, 40, 80, and 120 μM added $ZnCl_2$. Protein concentration was determined by amino acid analysis (Bidlingmeyer et al., 1984), and the mean residue ellipticity (MRE) was calculated (Adler et al., 1973) using a mean residue molecular weight of 115. Complete CD spectral analysis was performed using the algorithm of Provencher (Provencher & Glockner, 1981).

Analytical Ultracentrifugation. Analytical ultracentrifugal equilibrium analyses were performed with a Beckman XL-A analytical ultracentrifuge and an An-60Ti rotor. Two samples of VDR DBD in 5 mM Tris, 0.5 mM DTT, pH 8.0, prepared by buffer exchange from VDR DBD in TD-Zn (100 μM $ZnCl_2$), were utilized. Centrifugation was carried out at 20 °C. Rotor speed initially was 17 000 rpm (23000*g*). This was increased to 20 000 and 24 000 rpm (32000*g* and 46000*g*, respectively) serially after scans at each speed were complete. Scans were collected at 258 nm every 2 h for 12 h following the initial 12 h. Scans were compared to assure equilibrium had been reached. The partial specific volume of VDR DBD (ν = 0.718) was calculated using software supplied with the instrument.

Gel Shift Assays. To 1−3 pmol of ^{32}P-labeled double-stranded vitamin D response element (VDRE) dried under vacuum were added 9 μL of 50% (v/v) glycerol (15% final concentration), 6 μL of water or poly(dI-dC)·poly(dI-dC) (5 μg), and 15 μL of gel shift buffer (20 mM Hepes, 20% (w/v) glycerol, 0.1 M KCl, 0.2 mM EDTA, 20 μM $ZnCl_2$, 2.5 mM DTT, pH 7.9) alone or with VDR DBD or VDR DBD plus polyclonal antibody (made in rabbit to full-length hVDR) or with polyclonal antibody alone. The final volume of the reaction mixture was 30 μL. The mixture was placed on ice 10 min after addition of the reaction mixture to the labeled probe and then incubated at 30 °C for 20 min. The mixture was loaded onto 8% acrylamide gels made with 1×

running buffer [27 mM Tris-HCl pH 7.5, 13.2 mM sodium acetate, pH 7.0, 0.5 mM EDTA, pH 8.0 (final pH ~7.5 at 20 °C)] with 2.5% glycerol. The gels were prerun for 20 min at 150 V immediately before loading. Following loading the gels were run for 50 min at 100 V and then at 300 V for the remainder of the run (duration, ca. 2 h). The gels were dried and visualized with Kodak X-OMAT HR or BIOMAX MR film.

VDRE Oligonucleotides. The following VDRE oligonucleotides were used. mouse osteopontin, 5′ GCTCGGGTAG**GGTTCA**CGA**GGTTCA**CTCGACTCG3′; DR3, 5′ GCTCGGGTAG**AGGTCA**AGG**AGGTCA**CTCGACTCG 3′; DR3′, 5′ GCTCGGGTAG**AGTTCA**AGG**AGTTCA**CTCGACTCG 3′; human osteocalcin, 5′ GCTCGGGTAG**GGGTGA**CTCACC**GGGTGA**ACG**GGGGCA**TCTCGACTCG 3′; and Random, 5′ GCTCGGGTAGCTAATCCGTTTCGAGCTCGACTCG 3′.

In each case the complementary strand was synthesized. Sequences in bold and underlined are the vitamin D response element half-site hexamers. Sequences only underlined are half-site hexamers which were altered to make a randomized DNA sequence to destroy the VDRE half-site.

Radiolabeling of VDRE Probes. The double-stranded vitamin D response elements were formed by boiling equimolar amounts of the two oligonucleotides (100 pmol of each) for 5 min in 1× kinase buffer (85 mM Tris, 6 mM $MgCl_2$, 125 mM KCl, pH 7.6). The sample was cooled to ~30 °C over 50 min. β-Mercaptoethanol was added to 2 mM and 25 units of T4 polynucleotide kinase was added. Water was added to bring the volume to 50 μL. The mixture was added to 15 μL of dried γ^{32}P-ATP (3000 Ci/mmol) and placed at 37 °C in a water bath for 1 h. EDTA (2 μL, 0.5 M) was added to stop the reaction and the sample was then placed on ice.

Nuclear Magnetic Resonance Analyses. NMR data were acquired at 298 K on a Bruker AMX500 NMR spectrometer equipped with a 5 mm triple resonance inverse gradient probe. Standard pulse sequences and phase cycling were employed to record homonuclear ^{1}H one dimensional (1D) and two dimensional (2D) spectra in H_2O:D_2O (9:1). WATERGATE was used for water suppression. Spectra were recorded using water compensated NMR tubes with ~180 μL of sample volume (Shigemi Co. LTD, Tokyo, Japan, and Pittsburgh, PA). Experimental parameters are given in the figure captions. Oligonucleotides used for NMR studies were specific DNA, osteopontin VDRE 19mer (sense strand); half-sites are underlined in bold: 5′ IC**GGTTCA**CGA**GGTTCA**GA 3′; antisense strand, 5′ CTCTGAACCTCGTGAACCG 3′; nonspecific DNA, random 34mer (see Materials & Methods, VDRE Nucleotides).

RESULTS

Expression, Purification, and Characterization of the DNA Binding Domain of the Vitamin D Receptor. The DNA binding domain (DBD) of the human vitamin D receptor (VDR) and flanking naturally occurring amino-terminal and carboxyl-terminal sequences (residues 1−110 in VDR) were expressed as a fusion protein with glutathione-S-transferase (GST) in an *E. coli* expression system at low temperature (20 °C). This approach has previously been employed to obtain soluble VDR ligand binding domain (Craig & Kumar, 1996). The sequence of the DNA encoding the DNA binding domain of the VDR, flanking 5′ vector derived sequence regions and the corresponding protein sequence are shown in Figure 1. Circled are nine cysteines of which all but the final one act as zinc ligands in zinc finger regions of other proteins (Berg & Shi, 1996). The DNA insert encoding the fusion protein had the appropriate sequence on DNA sequencing. The fusion protein eluted from glutathione sepharose with 25 mM glutathione (reduced), 120 mM NaCl, 10 mM DTT, 50 mM Tris, pH 8 buffer. Addition of NaCl to the elution buffer was necessary for rapid and optimal elution of fusion protein from the resin. The fusion protein was cleaved with thrombin to yield the 1−110 VDR protein with a Gly−Ser dipeptide derived from the thrombin cleavage sequence added to the N-terminus. The mixture of the 1−110 VDR protein (VDR DBD) and glutathione-S-transferase was purified by Mono S ion-exchange chromatography. This was made possible by the unusually high (calculated) pI of the protein of 10.6 (calculated by MacVector sequence analysis software, Oxford Molecular Group, PLC). Highly purified fractions of VDR DBD eluted at ~0.4 M NaCl during Mono S column chromatography following wash steps at lower ionic strength (see Materials and Methods). Figure 2 shows an SDS−PAGE gel of the final Mono S purified VDR DBD (lane B). No other proteins were visible on staining with Coomassie blue. Minor contaminating bands representing <5% were seen on silver staining of similar gels (data not shown). The VDR DBD was recognized by a polyclonal antibody raised in rabbit to full-length VDR (Kumar et al., 1992) and was seen as a single band on a Western blot after peroxidase/diamino benzidine staining of SDS−PAGE gels transferred to nitrocellulose (data not shown). The purified protein had the appropriate composition as determined by amino acid analysis. As indicated in Figure 1, the VDR DBD protein was sequenced beginning from the amino-terminal end and from carboxyl-terminal end of the molecule. Sequencing beginning at the amino-terminus yielded the correct unambiguous amino acid sequence for residues 1−57. Sequencing beginning at the carboxyl-terminus of the molecule gave a sequence of nine amino acids (VDR amino acids 110−102) consistent with that expected for authentic VDR DBD.

ESI-MS of the VDR-DBD apo-protein demonstrated a M_r of 12 819 (Figure 3A). The expected molecular mass of the apo-VDR DBD is 12 819 (see Figure 3). No VDR DBD oligomers were detected. Lys-C protease digests of VDR DBD were analyzed by MALDI-MS as shown in Table 1. MALDI-MS demonstrated appropriate masses for peptides expected to be derived from VDR DBD from most regions of the protein.

The VDR DBD protein showed complete solubility at 4 °C at pH 8 (50 mM Tris, 10 mM DTT, pH 8.0, at 20 °C) and at pH 5.5 (25 mM sodium acetate, 10 mM DTT, pH 5.5) at millimolar concentrations but became insoluble at intermediate pHs. Severely decreased solubility was noted at mM protein concentrations on increasing pH from 5.5. Removal of zinc from the VDR DBD with EDTA resulted in precipitation of the majority of the protein at pH 5.5. The protein at pH 8, however, retained significant solubility when made zinc-free using EDTA.

Zinc Binding Stoichiometry of the VDR DBD. Initial studies on the ability of VDR DBD to bind zinc were carried out using ICP-MS following dialysis of protein in TD-Zn (100 μM $ZnCl_2$) buffer against TD buffer. Amino acid

Table 1: Matrix-Assisted Laser Desorption/Ionization-Mass Spectrometry (MALDI-MS) of Lys-C Protease Digests of the DNA Binding Domain of the Human Vitamin D Receptor (VDR DBD). Measured vs Predicted Fragment M_r[a]

MALDI-MS data measured MW (M_r)	average predicted MW of fragments (identity of Lys-C fragment)
788.8	790.0 (aa 106−111)
1027.6	1029.2 (aa 48−55)
1109.0	1111.4 (aa 85−93)
1506.3	1507.7 (aa 94−105)
1615.1	1616.8 (aa 73−84)
1801.3	1803.0 (aa 58−72)
5135[b]	5157.6 (aa 1−47)

[a]MALDI-MS of VDR DBD and of protease Lys-C digests of VDR DBD was carried out in order to characterize the protein. Intact VDR DBD in 50 mM NH_4HCO_3, pH 7.5, or VDR DBD Lys-C digests, with either α-cyano 4-hydroxycinnamic acid or 3,5 dimethoxy-4-hydroxy-cinnamic acid as matrix were subjected to MALDI-MS, using a nitrogen laser at 337 nm and a Braker Biflex mass spectrometer throughout. VDR DBD, with reduction and alkylation, was digested with Lys-C protease in 100 mM Tris-HCl, pH 8.25, for 3 h at 37 °C. Fragment aa 56−57 and aa 112 were not detected. Note that in this table the NH_2-terminus of the protein has two additional amino acids left following thrombin digestion from the GST-fusion protein. The construct contains 112 amino acid residues. The native DNA binding domain shown in Figure 1 has 110 amino acid residues. [b] This response is a broad peak. The precise identity is uncertain but it is in the right mass range to repesent the N-terminal peptide.

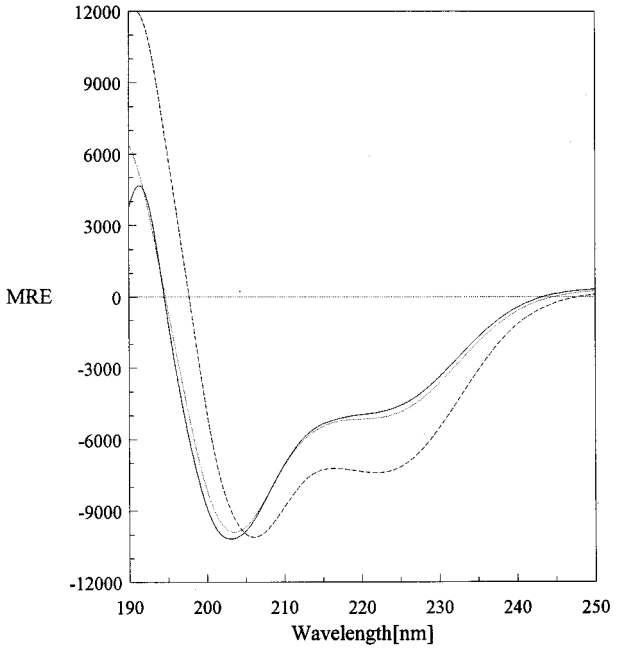

FIGURE 4: Circular dichroism spectra of VDR DBD. The CD spectra of the VDR DBD in the presence of 0 (solid line), 40 (dotted line), and 80 (dashed line) μM added $ZnCl_2$ are shown. Protein concentration was 29 μM.

analyses were performed to determine protein concentrations. Zinc:protein stoichiometries averaged 3.7 ± 0.5 (mean ± SD, $n = 5$) mol of zinc/mol of VDR DBD by this method after 4 days of dialysis. Zinc concentrations in final dialysis buffer were below the limits of detection. The VDR DBD in TD-Zn (100 μM $ZnCl_2$) was also analyzed following gel filtration with TD buffer, and yielded stoichiometries of 4.04 ± 0.15 (mean ± SD, $n = 3$) mol of zinc/mol of protein. When stoichiometries of zinc binding were measured following Mono S chromatography performed in the absence of added zinc, values of 2.45 ± 0.05 (mean ± SD, $n = 3$) mol of zinc/mol of VDR DBD were measured.

The zinc binding of the VDR DBD was also determined by electrospray ionization-mass spectrometry (ESI-MS) of the protein. Figure 3A shows the results of the deconvoluted spectrum of VDR DBD without zinc. The primary ion peak of mass (M_r) 12 819 Da corresponds to the expected mass for apo-VDR DBD (12 819 Da). During the course of examining the VDR DBD by ESI-MS, the protein has shown the propensity to adduct various species which can be removed by denaturing the protein. Although the identity of these products is not known, they do not appear to affect Zn^{2+} binding to the protein (Veenstra et al., 1997b). Figure 3B shows the deconvoluted spectrum of the VDR DBD dialyzed extensively against 4 mM NH_4HCO_3 and 1 mM DTT, pH 8.3. The major peak at $M_r = 12\,945$ Da corresponds to protein with two bound Zn^{2+}. The apo-VDR DBD is visible as the peak at $M_r = 12\,819$ Da. The one zinc-bound form of VDR DBD is visible at $M_r = 12\,882$. Figure 3C shows the deconvoluted spectrum of the protein in a solution containing a 50-fold molar excess of zinc. Mass assignments corresponding to the apo-protein ($M_r = 12\,819$ Da) and protein with 1 Zn^{2+} ($M_r = 12\,882$ Da), 2 Zn^{2+} ($M_r = 12\,945$ Da), 3 Zn^{2+} ($M_r = 13\,008$ Da), 4 Zn^{2+} ($M_r = 13\,071$ Da), 5 Zn^{2+} ($M_r = 13\,134$) and 6 Zn^{2+} ($M_r = 13\,197$) are observed. Treatment of zinc-liganded VDR DBD with EDTA, followed by the addition of excess zinc, gave a mass spectrum similar to that observed with Zn-liganded VDR DBD suggesting that Zn^{2+} could be reversibly removed from and added back to the protein (data not shown).

Circular Dichroism Spectroscopy of VDR DBD in the Absence and Presence of Zn^{2+}. Changes in the secondary structure of the VDR DBD upon the addition of zinc were measured by circular dichroism (CD) spectroscopy (Figure 4). The spectra of the VDR DBD (29 μM) upon the addition of Zn^{2+} to the protein in the apo-form in a low ionic strength pH 5.5 buffer (25 mM sodium acetate, 1 mM DTT, 10 μM EDTA, pH 5.5) are shown in Figure 4. Little change in the CD spectra of the protein was observed between 0 and 40 μM $ZnCl_2$ added. However at 80 μM $ZnCl_2$ (~70 μM free Zn^{2+}), a significant change in the conformation occurred within the protein. No change in the CD spectrum of the protein was observed at higher $ZnCl_2$ concentrations (data not shown). Analysis of the mean residue ellipticity (MRE) curves found the apo-VDR DBD to contain 16% α-helix, 56% β-strand, 23% β-turn, and 6% random coil. The Zn^{2+}-bound protein contained 27% α-helix, 39% β-strand, 23% β-turn, and 11% random coil. The addition of EDTA to the measuring curvette containing zinc-bound protein reversed the effects observed by the addition of $ZnCl_2$. The conformational changes within the VDR DBD upon the addition of $ZnCl_2$ were shown to be Zn^{2+}-specific, as the addition of $MgCl_2$ to the protein had no effect on the CD spectrum of the protein.

Analytical Ultracentrifugation of VDR DBD. In order to determine the oligomerization state of zinc replete VDR DBD, analytical ultracentrifugal analyses were carried out to equilibrium. In low ionic strength (5 mM Tris, 0.5 mM DTT) pH 8.0 buffer, at 20 °C, the VDR DBD was found to exist as a monomer in the 0.04−0.1 mM concentration range. There were no indications of multimeric species. Analytical runs at multiple speeds and protein concentrations gave similar results, showing a single monomer species with a calculated mass of 12351 ± 259 Da (±SD, $n = 5$).

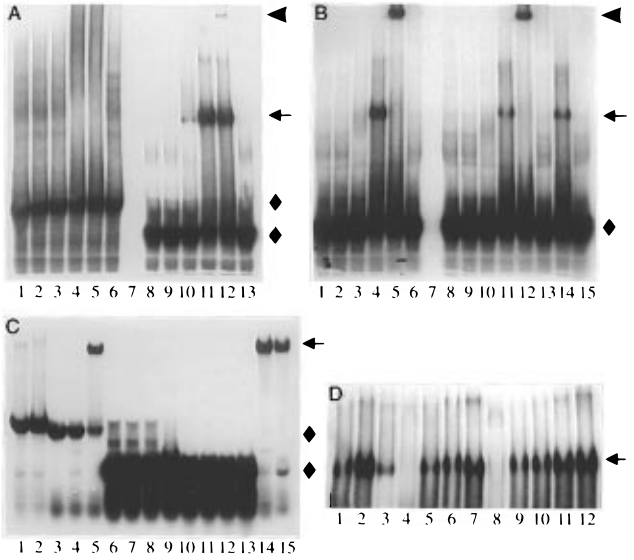

FIGURE 5: Gel shift analyses of VDR DBD binding to vitamin D response elements: 1−3 pmol double-stranded VDRE ^{32}P-labeled probe was dried under vacuum. VDR DBD (15 μL) diluted in reaction buffer (20 mM HEPES, pH 7.9, 20% (v/v) glycerol, 0.1 M KCl, 0.2 mM EDTA, and 2.5 mM dithiothreitol) was combined with glycerol (25%) final and H_2O to 30 μL final volume. In each panel the gel-shifted VDR DBD [^{32}P]VDRE complex is labeled with a left arrow. The antibody super shifted complex is labeled with a left arrowhead, and unbound probe is labled with a solid diamond. (A) Osteocalcin (OC) and osteopontin (OP) VDRE binding by the DBD. Lanes 1−6, OC VDRE. Lanes 8−13 OP VDRE. Lanes 1 and 8, VDRE probe only. Lanes 2−4 and 9−11, increasing DBD ~1, 10, and 100 pmol. Lanes 5 and 12, 100 pmol of DBD with polyclonal antibody to full-length VDR. Lanes 6 and 13, No VDR DBD; polyclonal antibody alone. (B) DR3′ and DR3 VDREs binding by the DNA DBD. Lanes 1−6, DR3′ VDRE. Lanes 8−15, DR3 VDRE. Lanes 1 and 8, VDRE probe only. Lanes 2−4 and 9−11, increasing DBD ~1, 10, and 100 pmol. Lanes 5 and 12, 100 pmol of DBD with polyclonal antibody. Lanes 6 and 13, No VDR DBD; polyclonal antibody alone. Lane 14, 100 pmol of DBD + 20 pmol of 105−427 hVDR (ligand binding domain; Craig & Kumar, 1996). Lane 15, 20 pmol of 105−427 hVDR without DBD. (C) Ability of single-stranded oligonucleotides from OP VDRE to bind to VDR DBD. Lanes 1 and 2, c-Fos VDRE. Lanes 3−5, OP VDRE. Lanes 6−9, single-stranded OP VDRE (sense strand). Lanes 10−13, single-stranded OP VDRE (anti-sense strand). Lanes 14 and 15 competition of unlabeled single-stranded OP VDRE oligonucleotides with labeled double-stranded OP VDRE; unlabeled single-stranded sense strand lane 14; unlabeled single-stranded anti-sense strand lane 15. Lanes 1, 3, 6, and 10, probe only. Lanes 2, 14, and 15, 100 pmol of DBD. Lanes 4 and 5, 10 and 100 pmol of DBD, respectively. Lanes 7−9 and 11−13, 1, 10, and 100 pmol of DBD, respectively. (D) Competition of unlabeled OP or osteocalcin VDRE or randomized double-stranded DNA with labeled OP VDRE for formation of VDRE/DBD shifted complex. Labeled OP VDRE (~1 pmol) and ~100 pmol of DBD were used to form a gel-shifted complex. Lanes 1−4, increasing amounts of unlabled OP VDRE. Lanes 5−8, increasing amounts of unlabled OC VDRE. Lanes 9−12, increasing amounts of unlabeled randomized DNA sequence. Unlabeled VDRE DNA (0, 1, 25, or 250 pmol) was used in each case.

VDR DBD: Vitamin D Response Element Interactions. Structural/functional competency of the zinc replete VDR DBD to form *in vitro* complexes with vitamin D response elements (VDREs) is shown in Figure 5, panels A−D. Radiolabeled mouse osteopontin (OP), human osteocalcin (OC), or synthetic response elements DR3 or DR3′ (see Materials and Methods) were incubated and run with the VDR DBD on 8% nondenaturing polyacrylamide gels. The VDR DBD bound to the OP VDRE (Figure 5A) to give an intense gel-shifted complex (lanes 10−12, arrow). Polyclonal antibody (to full-length VDR) addition gave a supershifted complex (arrowhead). A mixture of VDR DBD and OC VDRE, on the other hand (lanes 2−5), gave no distinct gel-shifted complexes. The DR3 and DR3′ probes also gave distinct gel-shifted bands (Figure 5B) and antibody supershifted bands with VDR DBD and were similar in sequence to OP VDRE (half sites of AGGTCA and AGTTCA for DR3 and DR3′, respectively, versus GGTTCA for OP VDRE halfsite). Addition of the bacterially expressed ligand binding domain of VDR had no effect on the OP VDRE gel shift (lanes 14 and 15). No gel-shifted complex of single stranded DNA (ssDNA) probes (oligonucleotides from OP VDRE) were observed (Figure 5C, lanes 6−13), nor were they able to compete for binding when combined with (double-stranded) OP VDRE (lanes 14 and 15). Inability of VDR DBD to form a gel-shifted complex with c-Fos VDRE is shown in lanes 1 and 2, Figure 5C (Candeliere et al., 1996).

Specificity of complex formation of the OP VDRE and VDR DBD is shown (Figure 5D). VDR DBD was combined with 0, 1, 25, or 250 pmol of unlabeled OP or OC VDRE or randomized DNA (see Materials and Methods) and then incubated with ~1 pmol of labeled VDRE. The ability of unlabeled VDREs or random DNA to compete for binding with the labeled VDRE probe was determined by the presence of a gel-shifted band on nondenaturing PAGE. As can be seen in lanes 1−4, increasing amounts of cold unlabeled double-stranded OP VDRE competed quite well with the labeled probe at 25 pmol and completely at 250 pmol. The unlabeled OC VDRE was less competent at competing for binding with the OP VDRE since 25 pmol showed no discernible reduction in intensity of the gel-shifted band (lane 7), although 250 pmol (lane 8) effectively competed off the probe. As a control, a double-stranded DNA fragment with contextual sequences similar to the OP VDRE, but with the two half-sites randomized such that they no longer showed similar sequence to the OP VDRE half-site was used. In this case, even the highest amount of the random DNA added, 250 pmol (lane 12), showed no noticeable reduction in intensity of the gel-shifted band.

Nuclear Magnetic Resonance Studies of VDR DBD. Structural events in VDRE/VDR DBD were next examined by NMR (Figures 6 and 7). Figure 6 shows protein and DNA spectra. It compares the linear combination (4:1) spectrum of the separately recorded spectra of the protein and DNA with the spectrum of their 4:1 mixture. Upon addition of DNA to the protein, DNA lines in the amino range (11−16 ppm) are shifted for specific DNA (Figure 6A) indicating complex formation, whereas DNA lines of nonspecific DNA remain unshifted (Figure 6B).

Appearance of amide/amide cross-peaks in NOESY spectrum, Figure 7, indicate the presence of secondary structure in the protein. However, a relatively modest spread and small number of amide/amide NOESs suggest that certain portions of the protein may be unstructured or too flexible on the NMR time scale.

DISCUSSION

The use of low-temperature expression of a GST-fusion protein coupled with Mono S chromatography allowed us to prepare pure VDR DBD. The measurement of the number of zinc ions bound to the protein following dialysis or gel

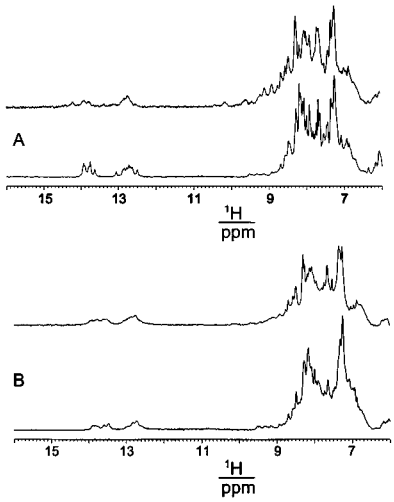

FIGURE 6: Linear combination (4:1) ^{1}H NMR of the separately recorded spectra of VDR DBD and the specific DNA (OP VDRE) (A, lower spectrum). Spectrum of the protein and specific DNA mixture (A, upper spectrum). The same is presented in panel B for nonspecific DNA (randomized double-stranded DNA). Protein concentration ~0.2 mM, 512 scans, 25 °C.

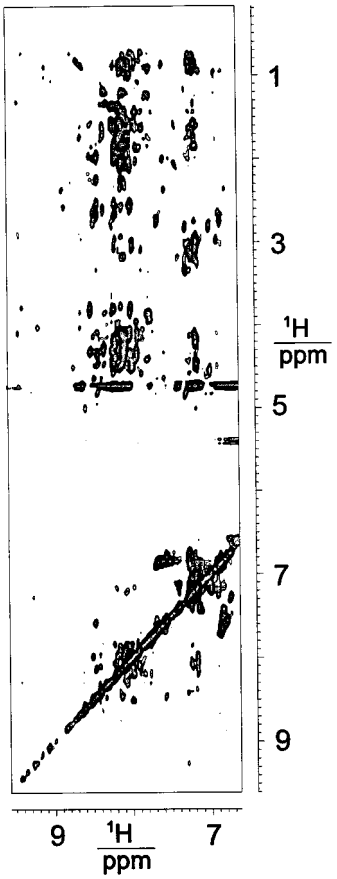

FIGURE 7: Amide-to-aliphatic region of the NOESY spectrum of 0.2 mM VDR DBD at 25 °C in 9:1 H_2O:D_2O mixture; spectrum is recorded with mixing time of 250 ms, 512 t_1 increments with 1024 complex T_2 points and 128 scans each. Residual water signal is removed by 3-9-19 WATERGATE sequence with 130 μs pulse spacing. Time domain data are zero filled and filtered with 80° shifted square sinebell window in both domains yielding real spectrum of 1024 × 1024 points.

filtration gave zinc/protein stoichiometries of ~4. Measurement of zinc/protein stoichiometries in Mono S column fractions collected in the absence of zinc demonstrated ~2 mol of zinc/mol of protein.

We used electrospray ionization-mass spectrometry (ESI-MS) as another approach to determine the number of zinc ions bound/mol of VDR DBD (Figure 3). ESI-MS of the VDR DBD prepared so as to remove zinc gave a primary mass of VDR DBD of 12 819 Da (Figure 3A), which is in excellent agreement with the calculated mass for the zinc free protein (12 819 Da). ESI-MS of the VDR DBD prepared with zinc but exchanged into 4 mM NH_4HCO_3 buffer without zinc gave a mass corresponding to the protein bound to 2 mol of zinc. When excess zinc is added to the protein (50:1), a minimum of 2 additional mol of Zn^{2+} (total = 4−6) are bound to 1 mol of protein. The observed mass of 13 071 Da compares favorably to the calculated mass of the four zinc VDR DBD of M_r = 13 072 Da. These additional zinc sites probably represent lower affinity binding sites. These ESI-MS results are consistent with the zinc/protein stoichiometry of ~4 mol of zinc/mol of protein seen when zinc was measured directly by ICP-MS after limited dialysis or gel filtration, and of ~2 mol of zinc/mol of protein observed following chromatography in zinc-free buffer. To date, the only other measurements of metal binding to other steroid/thyroid superfamily receptors by ESI-MS have yielded 0−2 zincs/molecule (Allen & Hutchens, 1992) and 0, 3, and 4 bound Cu/molecule (Hutchens et al., 1992) for the estrogen receptor DBD. Our results are consistent with the presence of two high affinity Zn^{2+} binding sites in VDR DBD, and the presence of a minimum of two additional sites of lower affinity which appear when large amounts of Zn^{2+} are added to the protein. The value of two moles of Zn^{2+}/mol of VDR DBD would be expected for 2-Cys_2Cys_2-zinc finger peptides (Berg & Shi, 1996) which have two zinc binding sites comprised of eight cysteines. Values of 2.3 ± 0.2 zinc ions per glucocorticoid receptor (GR) DBD were reported and 2.1 ± 0.2 cadmium ions/molecule when this protein was Cd^{2+} reconstituted (Freedman et al., 1988; Pan et al., 1990). Three zinc ions/molecule were reported for the GR DBD as well (Pan et al., 1990).

The results demonstrating at least 4 zinc ions/molecule VDR DBD at higher concentrations of zinc are greater than those expected for 2-Cys_2Cys_2-zinc finger proteins which usually have only two sites for zinc binding (Evans, 1988; Berg & Shi, 1996). Which VDR amino acid residues constitute the binding sites for the 2−4 additional zinc ions/molecule VDR DBD are unknown. Upon the basis of X-ray crystallographic and NMR structures of other steroid/thyroid superfamily members, VDR DBD could reasonably be expected to have one Cys, probably Cys_{86}, not participating in a "zinc finger". In addition, there are two His residues in VDR DBD; histidines are well-known for binding zinc in biological systems (Sundberg & Martin, 1974; Berg & Shi, 1996). Whether methionines are involved as proposed for the third, low-affinity, zinc binding site seen with the GR, (Pan et al., 1990) or whether the unusually high calculated pI of the protein (pI = 10.6) has a role in zinc binding is unknown. Methionines are well-known for acting as metal liganding residues in metalloenzymes (Chakrabarti, 1989; Christianson, 1991) but typically for metals other than zinc. Other residues might be involved in Zn^{2+} binding but their relevance to VDR DBD is not known (Christianson, 1991; Coffer et al., 1996; Postal et al., 1985; Springman et al., 1995; Surovoy et al., 1992; Berg & Shi, 1996).

In order to quantify protein secondary structural parameters with VDR DBD on metal binding, circular dichroism was

utilized. On addition of zinc to a concentration which would give an ~1:1 zinc:protein stoichiometry (Figure 4; dotted line), there was no change in structure as seen from CD. When the zinc:protein ratio was increased to ~2:1 (Figure 4; dashed line) (~70 μM free zinc) (Dean, 1995), a ratio that would be sufficient to saturate the two putative "zinc fingers", there was a large change in structure which results in a ~11% increase (from 16 to 27% calculated values) in α-helical content. Removal of zinc from zinc-replete protein by subsequent addition of EDTA resulted in a reversion of the protein to a structure seen in the apo-protein. These results are consistent with our experiments using ESI-MS in which VDR DBD was shown to undergo a large conformational change upon the addition of two Zn^{2+} ions to each mole of protein as evidenced by significant change in the mass to charge ratio distribution. Smaller additional changes in the mass to charge ratio distribution were observed when additional Zn^{2+} was added to protein (Veenstra et al., 1997a,b).

As indicated by the results and competition assay, the zinc replete VDR DBD forms a complex with osteopontin (OP) and similar VDREs (Figure 5). Some interaction, although a weaker interaction than with OP VDRE, is probably occurring with osteocalcin (OC) VDRE since an antibody-supershifted band is sometimes seen and the OC VDRE competes with OP VDRE for binding to VDR DBD (Figure 5D). Such an affinity for OP and OC VDREs has been seen before with VDR DBD (Freedman & Towers, 1991; Nishikawa et al., 1993). The ability of VDR DBD to interact specifically with VDREs in the absence of accessory proteins to form a structural entity attests to the inherent specificity built into these DNA and protein sequences. The particular *in vitro* stability (e.g., OC vs OP VDRE) is not, however, necessarily a predictor of *in vivo* function (Ohyama et al., 1996). We are currently examining VDR DBD−VDRE interactions by ESI-MS. At present, no complexes have been observed although Cheng et al. (1996) have had success with single-stranded DNA−DNA binding protein interactions by ESI-MS.

The VDR DBD was found to interact similarly with the DR3 and DR3′ response elements and to the OP VDRE (Figure 5, panels A and B). This contrasts with previous report(s) in which DR3 was not bound or showed minimal binding for a DR3 VDRE (Freedman & Towers, 1991; Nishikawa et al., 1993). Whether the difference lies in the method of protein preparation, the binding conditions employed or whether the additional amino- or carboxyl-terminal VDR sequence incorporated into our construct are responsible is unknown. Recently, in work with the thyroid hormone receptor (Judelson & Privalsky, 1996), it was proposed the N-terminus of steroid receptors is critically involved in DNA recognition and alters the conformation of receptor domains. Thus, a construct with an intact N-terminus (such as the VDR DBD used in this study) might interact differently with a DNA response element than a construct containing only immediate "zinc finger" amino acids. Protein sequence extending C-terminal to the putative zinc finger region have also been implicated in DNA recognition (Wilson et al., 1992; McBroom et al., 1995).

The ability of zinc replete VDR DBD to interact specifically with a VDRE was demonstrated in an unambiguous way by NMR in Figure 6. Specific changes in the OP VDRE DNA lines (11−16 ppm) (Figure 6A) showed specific structural changes were occurring in the DNA on protein binding (11−16 ppm) while lines from randomized double-stranded DNA (Figure 6B) did not change. Other changes seen are difficult to interpret since they did not exclusively represent only protein or DNA lines. Characteristics of the VDR DBD without DNA present were revealed by proton 2D NOESY spectra (Figure 7). Under conditions where VDR DBD binds only 2 mol of zinc/mol of protein, protein structure was present indicating only two zinc ions/VDR DBD molecules are required in order to establish the protein structure, but also that certain regions may be unstructured or more flexible, on the NMR time scale.

In conclusion, highly purified preparations of the DBD of human VDR have been shown to bind two zinc atoms per protein molecule when prepared in low zinc concentrations, and four zinc atoms per molecule of protein in the presence of excess zinc. Zinc has been shown to induce structural changes in the VDR DBD which are likely to be functionally important. The zinc-replete VDR DBD interacts to form *in vitro* specific complexes with VDREs, and this specific interaction is visible by changes in both the DNA and possibly the protein by proton NMR. Additional studies should clarify the nature of the zinc binding sites on the VDR DBD.

ACKNOWLEDGMENT

We would like to thank Benjamin Madden and the Mayo Protein Core Facility for amino acid compositions and protein sequencing, Dr. David Nixon and the Mayo Metals Laboratory for measurements of zinc, and Dr. C. T. McMurray for assistance with analytical ultracentrifugation.

REFERENCES

Adler, J. A., Greenfield, N. J., & Fasman, G. D. (1973) *Methods Enzymol. 27*, 675−735.
Allen, M. H., & Hutchens, T. W. (1992) *Rapid Commun. Mass Spectrom. 6*, 308−312.
Asubel, F. M., *et al.* (1995) *Current Protocols in Molecular Biology* (1995) John Wiley and Sons, NY.
Berg, J. M., & Shi, Y. (1996) *Science 271*, 1081−1085.
Bidlingmeyer, B. A., Cohen, S. A., & Tarvin, T. L. (1984) *J. Chromatogr. 336*, 93−104.
Candeliere, G. A., Jurutka, P. W., Haussler, M. R. H., & Starnaud, R. (1996) *Mol. Cell. Biol. 16*, 584−592.
Carlberg, C. (1996) *Endocrine 4*, 91−105.
Carlberg, C., Bendik, I., Wyss, A., Meier, E., Sturzenbecker, L. J., Grippo, J. F., & Hunziker, W. (1993) *Nature 361*, 657−660.
Chakrabarti, P. (1989) *Biochemistry 28*, 6081−6085.
Cheng, X., Harms, A. C., Goudreau, P. N., Terwilliger, T. C., & Smith, R. D. (1996) *Proc. Natl. Acad. Sci. U.S.A. 93*, 7022−7027.
Christianson, D. W. (1991) *Adv. Protein Chem. 42*, 281−355.
Coffer, A., Cavailles, V., Knowles, P., & Pappin, D. (1996) *J. Steroid Biochem. Mol. Biol. 58*, 467−477.
Craig, T. A., & Kumar, R. (1996) *Biochem. Biophys. Res. Commun. 218*, 902−907.
Darwish, H., & De Luca, H. F. (1993) *Crit. Rev. Eukaryotic Gene Expression 3*, 89−116.
Dean, J. A. (1995) in *Analytical Chemistry Handbook*, p 3.96, McGraw-Hill, New York.
Evans, R. M. (1988) *Science 240*, 889−895.
Freedman, L. P., & Towers, T. L. (1991) *Mol. Endocrinol. 5*, 1815−1826.
Freedman, L. P., Luisi, B. F., Korszun, Z. R., Basavappa, R., Sigler, P. B., & Yamamoto, K. R. (1988) *Nature 334*, 543−546.
Freedman, L. P., Cheskis, B., Lemon, B., Liu, M., & Towers, T. L. (1994) in *Vitamin D* (Norman, A. W., Bouillon, R., & Thomasset, M., Eds.) pp 217−225, W. de Gruyter & Co., Berlin.

Haussler, M. R., Jurutka, P. W., Hsieh, J.-C., Thompson, P. D., Selznick, S. H., Haussler, C. A., & Whitfield, G. K. (1995) *Bone 17*, 33S−38S.

Holick, M. F. (1995) *Bone 17S*, 107S−111S.

Hsieh, J.-C., Nakajima, N., Galligan, M. A., Jurutka, P. W., Haussler, C. A., Whitfield, G. K., & Haussler, M. R. (1995) *J. Steroid Biochem. Mol. Biol. 53*, 583−594.

Hutchens, T. W., Allen, M. H., Li, C. M., & Yip, T.-T. (1992) *FEBS Lett. 309*, 170−174.

Innis, M. A., Gelfan, D. H., Sninsky, J. J., & White, T. J. (1990) *PCR Protocols: A Guide to Methods and Applications*, Academic Press, San Diego, CA.

Judelson., C., & Privalsky, M. L. (1996) *J. Biol. Chem. 271*, 10800−10805.

Kliewer, S. A., Umesono, K., Mangelsdorf, D. J., & Evans, R. M. (1992) *Nature 355*, 446−449.

Kumar, R. (1990) *J. Am. Soc. Nephrol. 1*, 30−42.

Kumar, R. (1991) *Kidney Int. 40*, 1177−1189.

Kumar, R., Schaefer, J., & Wieben, E. (1992) *Biochem. Biophys. Res. Commun. 189*, 1417−1423.

Laemmli, U. K. (1970) *Nature 227*, 680−685.

Lowe, K. E., Maiyar, A. C., & Norman, A. W. (1992) *Crit. Rev. Eukaryotic Gene Expression 2*, 65−109.

Mangelsdorf, D. J., Thummel, C., Beato, M., Herrlich, P., Schutz, G., Umesono, K., Blumberg, B., Kastner, P., Mark, M., Chambon, P., & Evans, R. M. (1995) *Cell 83*, 835−839.

McBroom, L. D. B., Flock, G., & Giguere, V. (1995) *Mol. Cell Biol. 15*, 796−808.

Nishikawa, J.-I., Matsumoto, M., Sakoda, K., Kitaura, M., Imagawa, M., & Nishihara, T. (1993) *J. Biol. Chem. 268*, 19739−19743.

Ohyama, Y., Ozono, K., Uchida, M., Yoshimura, M., Shinki, T., Suda, T., & Yamamoto, O. (1996) *J. Biol. Chem. 271*, 30381−30385.

Pan, T., Freedman, L. P., & Coleman, J. E. (1990) *Biochemistry 29*, 9218−9225.

Pharmacia Biotech Inc. (1994) 2nd ed., *GST Gene Fusion System* (manual).

Pike, J. W. (1991) *Annu. Rev. Nutr. 11*, 189−216.

Postal, W. S., Vogel, E. J., Young, C. M., & Greenaway, F. T. (1985) *J. Inorg. Biochem. 25*, 25−33.

Provencher, S. W., & Glockner, J. (1981) *Biochemistry 20*, 33−37.

Sambrook, J., Fritsch, E. F., & Maniatis, T. (1989) *Molecular Cloning: A Laboratory Manual*, 2nd ed.; pp 5.68−5.69, Cold Spring Harbor Laboratory, Plainview, NY.

Sanger, F., Nicklen, S., & Coulson, A. R. (1977) *Proc. Natl. Acad. Sci. U.S.A. 74*, 5463−5467.

Schwabe, J W. R., & Rhodes, D. (1991) *Trends Biochem. Sci. 16*, 101−118.

Springman, E. B., Nagase, H., Birkedal-Hansen, H., & Van Wart, H. (1995) *Biochemistry 34*, 15713−15720.

Sundberg, R. J., & Martin, R. B. (1974) *Chem. Rev. 74*, 471−517.

Surovoy, A., Waidelich, D., & Jung, G. (1992) *FEBS Lett. 311*, 259−262.

Veenstra, T. D., Johnson, K. L., Tomlinson, A. J., Naylor, S., & Kumar, R. (1997a) *Biochemistry 36*, 3535−3542.

Veenstra, T. D., Johnson, K. L., Tomlinson, A. J., Craig, T. A., Kumar, R., & Naylor, S. (1997b) *J. Am. Soc. Mass Spec.* (submitted for publication).

Wilson, T. E., Paulsen, R. E., Padgett, K. A., & Milbrandt, J. (1992) *Science 256*, 107−110.

BI970561B